

Where Are The M Dwarf Disks Older Than 10 Million Years?

Peter Plavchan, M. Jura, & S. J. Lipsky[†]

UCLA Department of Physics and Astronomy; plavchan@astro.ucla.edu

† Now at Ball Aerospace

ABSTRACT

We present 11.7-micron observations of nine late-type dwarfs obtained at the Keck I 10-meter telescope in December 2002 and April 2003. Our targets were selected for their youth or apparent IRAS 12-micron excess. For all nine sources, excess infrared emission is not detected. We find that stellar wind drag can dominate the circumstellar grain removal and plausibly explain the dearth of M Dwarf systems older than 10 Myr with currently detected infrared excesses. We predict M dwarfs possess fractional infrared excess on the order of $L_{IR}/L_* \sim 10^{-6}$ and this may be detectable with future efforts.

Subject headings: stars: circumstellar matter – stars: late-type – stars: winds, outflows

1. INTRODUCTION

Until ~ 20 years ago, our knowledge of planets and their formation had been limited to our own solar system, with planets around other stars being the subject of fiction and hypothesis. With recent advances in instrumentation and detection capabilities, we are now confirming the existence of planetary systems around other stars. In 1983, the InfraRed Astronomical Satellite (hereafter IRAS) offered the first evidence of dusty debris, or debris disks, orbiting other stars (Zuckerman 2001). The dust is heated by the incident stellar radiation and re-emits this radiation in the infrared, which we can then detect as an “excess” of infrared flux. The first extra-solar planets were indirectly detected around a millisecond pulsar in 1993 by analysis of the pulsar timing (Wolszczan & Frail 1992). Finally, the first jovian planets around stars like our sun were discovered in 1995 through the characteristic “wobble” or radial velocity variations induced in the star (Mayor & Queloz 1995). Studying the evolution of these systems and their characteristics – both directly and indirectly – allow us to begin to answer fundamental questions about the existence of life in the universe.

M Dwarfs are the lowest mass, size, luminosity and temperature main sequence stars which comprise $\sim 70\%$ of the total number of stars in our galaxy (Mathioudakis & Doyle 1993). If planetary systems exist around M Dwarfs, they could represent the most abundant planetary systems in the galaxy. Thus, determining or constraining the abundance of exoplanetary systems around M Dwarfs is important.

About 15% of nearby main-sequence stars exhibit far-infrared excess characteristic of cold circumstellar dust, or debris disks analogous to our Kuiper belt (Habing et al. 2001). However, most M-type stars do not currently have detected infrared excesses despite several targeted and blind surveys (Song et al. 2002; Weinberger et al. 2004; Zuckerman 2001; Liu et al. 2004; Fajardo-Acosta et al. 2000). Reported $12\mu\text{m}$, $20\mu\text{m}$ and $25\mu\text{m}$ IRAS and ISO (Infrared Space Observatory) excess emission candidates have been largely demonstrated as false-positives when followed-up by smaller aperture ground-based observations (Zuckerman 2001; Song et al. 2002; Fajardo-Acosta et al. 2000; Aumann & Probst 1991).

We have performed a search for $12\mu\text{m}$ infrared excess around candidate M Dwarfs indicative of extrasolar zodiacal dust. The presence of such warm debris disks, analogous to the zodiacal dust in our own inner solar system, could be an indirect marker for the presence of parent bodies – rocky planetesimals, asteroids and comets that can generate dust.

We present selection criteria for our targets in Section 2, and we present our observations in Section 3. In Section 4, we present an analysis of the observations using stellar atmosphere models to estimate photospheric contributions to the observed infrared flux. We present a model for circumstellar grain removal for M dwarfs in Section 5 to explain our results and the dearth of M dwarfs older than 10 Myr with observed infrared excess. In section 6, we discuss the implications of this model and we present our conclusions in Section 7.

2. SAMPLE SELECTION

We constructed our sample from two selection criteria – youth and apparent $12\mu\text{m}$ excess. Our target list is given in Table 1.

2.1. Youth

Spangler et al. (2001) have found that for solar-type stars, the infrared excess varies as $t_*^{-1.76}$ where t_* is the age of the star. They present a simple model for asteroidal destruction to explain this result. Extrapolating from the infrared excess produced by our own zodiacal debris, if we can identify M type stars which are ~ 0.1 the age of the Sun ($t_* \sim 500$ Myr)

or younger, any existing infrared excess might be detectable with ground-based facilities. Similarly, Liu et al. (2004) estimated that the dust mass, M_d , varies as $t_*^{-0.5}$ to t_*^{-1} from debris disk masses estimated from sub-mm data, with a simple unweighted fit giving $M_d \propto t^{-0.7 \pm 0.2}$. Finally, from the lunar impact record one can infer that the amount of debris and resulting infrared excess can be significantly higher for young solar analogs (Chyba 1991). See Decin & Dominik (2003) for a re-examination of the time-dependence of the IR excess amplitude, which leads to a different conclusion than Spangler et al. (2001).

In order to identify young, nearby M-type stars, we have used the results for the β Pic moving group from Zuckerman et al. (2001) and the “rapid” rotators from the survey by Gizis et al. (2002) to identify three targets. The most obvious candidate in the β Pic moving group is GJ 3305 (Song et al. 2002) since AU Mic (GJ 803) is also member of this moving group and an M-type dwarf with an imaged debris disk (Kalas et al. 2004; Liu 2004). The estimated age of GJ 3305 is 12 Myr, or $3 \times 10^{-3} t_\odot$. From Gizis et al. (2002), GJ 3304 and GJ 3136 are “rapid rotator” stars with $v \sin i = 30 \text{ km s}^{-1}$, so these stars are likely younger than the Hyades and therefore about 0.1 the age of the Sun (Terndrup et al. 2000).

2.2. Apparent $12\mu\text{m}$ Excess

With the release of the 2MASS All Sky Survey, we cross-correlated this catalog with the IRAS Point Source and Faint Source Catalogues, similar and analogous to the work of Fajardo-Acosta et al. (2000). We used the volume complete 676-source M Dwarf sample of Gizis et al. (2002) and the 278-source dwarf K and M-type sample identified in Mathioudakis & Doyle (1993). There is moderate overlap between these two samples. We selected targets with unusually red K-[$12\mu\text{m}$] colors. We eliminated sources exhibiting a false color excess attributable to IRAS beam confusion, such as binaries or relatively bright nearby companions within $1'$. Additionally, with the exception of HU Del (GJ 791.2), known binary sources were discarded. Our most promising six targets were observed. With the exception of GJ 585.1, a K5 dwarf, the remaining five targets are M-type.

3. OBSERVATIONS

We present $11.7\mu\text{m}$ observations of nine late-type dwarfs obtained at the Keck I 10-meter telescope in December 2002 and April 2003. Table 1 lists the target stars, their distance, $11.7 \mu\text{m}$ observed photometry, $12 \mu\text{m}$ IRAS photometry, and derived $3\text{-}\sigma$ upper-limits on the infrared excess from synthetic spectral fitting. Table 2 lists the observations and integration

times. Figures 1 and 2 shows spectral fits, observations and available literature photometry.

These three targets selected for their youth – GJ 3136, GJ 3304 and GJ 3305 – were observed at Keck at $11.7\mu\text{m}$ using the Long Wavelength Spectrograph (LWS) in imaging mode in December 2002 (Jones & Puetter 1993). On-source integrations times for all three targets were two minutes. Standard IDL routines were used to reduce the data, and we wrote IDL routines to flux-calibrate the data.

For the particular observations in December 2002, it was discovered later by Varoujan Gorjian (Gorjian 2003, private comm.) and confirmed by Keck staff that a screw that adjusts a mirror in the LWS detector had come loose and fallen out. This allowed some movement of the optics as a function of telescope orientation during the time of our observations. However, we observed standards within $1'$ of our targets for GJ 3304 and GJ 3305, and all three targets and standards were observed at airmasses ≤ 1.2 . Nevertheless, this potentially adversely affected the calibrations used in our observations, especially for GJ 3136, introducing a systematic error. Thus, we treated the variance in the calibration of our standards as systematic errors rather than random, and adjusted our resulting uncertainties in our observations accordingly. The net result was to roughly double our final calibration uncertainties.

The six targets selected for their apparent IRAS $12\mu\text{m}$ excesses were observed at Keck using LWS at $11.7\mu\text{m}$ in April 2003, using the same reduction techniques described above. On source integration times ranged from 2 to 5 minutes. In the cases of G 203-047 and HU Del, target acquisition and identification was performed with NIRC (Keck Near Infra-Red Camera) K-band imaging (Matthews & Soifer 1994).

4. ANALYSIS

Photospheric flux was estimated by fitting PHOENIX NextGen stellar atmosphere models (Hauschildt et al. 1999) to available UBVR_IJHK_s photometry, taking into account effective bandpasses and photometric uncertainties in finding the minimum χ^2 in temperature and normalization. The JHK_s photometry were obtained from 2MASS All-Sky Survey and converted to flux densities based on the calibration by Cohen et al. (2003), outlined in the 2MASS Explanatory Supplement (Cutri et al. 2003, ch VI.4a). UBV and R-I photometry, when available, were obtained from the Gliese catalogue. R magnitudes, when available, were obtained from the USNO-A V2.0 catalogue queried through Vizier (Ochsenbein et al. 2000; Gliese & Jahreiss 1979, 1991; Monet et al. 1998). Correcting USNO-R to Landolt-R magnitudes did not affect our model SED fits. The IRAS $12\mu\text{m}$ flux densities were color-corrected

assuming blackbody emission, following the procedures outlined in the IRAS Explanatory Supplement (Beichman et al. 1988, ch.VI.C.3). The adopted color correction factors were chosen depending on the effective temperature T_{eff} of each star, with a typical value of ~ 1.41 .

PHOENIX Nextgen models were used to fit the observed photometry rather than a blackbody, since the stellar SEDs are very different from that of a blackbody (Song et al. 2002; Mullan et al. 1989). We assumed $\log g = 4.5$ and solar metallicity, as is typical for main-sequence stars in the solar neighborhood (D’Antona & Mazzitelli 1997; Drilling & Landolt 2000). Six of our nine targets are previously identified as flare stars, which primarily affect the U and B magnitudes during flaring. However, the exclusion of U and B band magnitudes in our SED fits did not alter the derived temperatures for our targets. Uncertainties in the predicted model flux at $11.7\mu\text{m}$ are derived from the resulting variance of the spectral fit as a function of the temperature ($\pm 100\text{K}$) and effective normalization ($\pm 5\%$) uncertainties around the minimum reduced χ^2 fit.

We find that the spectral models and photometric data are self consistent with one another, and consistent with no detected infrared excess at $11.7\mu\text{m}$ for all nine targets. Our derived effective temperatures are in agreement with published spectral types when available. We obtain an overall reduced χ^2 of the model fits to the data of 0.95, and on average the $3\text{-}\sigma$ upper limits correspond to a ratio of $F_{d,\nu}/F_{*,\nu} \sim 30\%$ at $11.7\mu\text{m}$, excluding GJ 4068. This ratio limit is typical for current ground-based mid-infrared observational capabilities; we are limited in our analysis by our photometric quality rather than model-fitting uncertainties.

4.1. Comments on the discrepancies between our ground-based observations and IRAS flux measurements.

IRAS did not detect GJ 3304, GJ 3305 and GJ 3136 in the Point Source and Faint Source Catalogues, but as one can see in Figure 1 our measurements at $11.7\mu\text{m}$ are consistent with the predicted photospheric emission. For GJ 4068, GJ 507.1, HU Del and GJ 585.1, we note that the color-corrected IRAS $12\mu\text{m}$ measurements are inconsistent with our $11.7\mu\text{m}$ measurements with a significance of $\sim 5.5\text{-}$, 3- , 2- , and $2.5\text{-}\sigma$ respectively. The IRAS $12\mu\text{m}$ measurements are also inconsistent with the predicted photospheric emission at the $\sim 9\text{-}$, 2.5- , 2- , and $3\text{-}\sigma$ respectively. It is unlikely that these discrepancies are due to the presence of Si emission in the IRAS $12\mu\text{m}$ bandpass, which would be missed by the LWS $11.7\mu\text{m}$ bandpass (Metchev et. al. 2004; Gaidos & Koresko 2004). For HU Del and GJ 4068 we suspect that this inconsistency is due to beam confusion from nearby sources, located ~ 1.0 and ~ 2.1 arc-minutes away, respectively. For GJ 507.1 and GJ 585.1, we suggest that the

inconsistencies are probably due to statistical fluctuations and the “Malmquist-bias” for stars near the detection threshold (Song et al. 2002).

For G 203-047 and GJ 729, we note that the color-corrected IRAS $12\mu\text{m}$ measurements and our $11.7\mu\text{m}$ measurements are both consistent with one another and the predicted model photospheric emission. Although G 203-047 and GJ 729 possessed unusually red K-[$12\mu\text{m}$] colors in our initial sample, this was not indicative of a true excess with subsequent modeling of their cool photospheres. For GJ 4068, the flux error is dominated by systematic error in our calibration rather than statistical uncertainties in the detection itself. Thus, we report a detection rather than an upper-limit. For HU Del, we note that it is a spectroscopic binary, which may account for the model spectral fit appearing to be slightly inconsistent with the literature photometry. Finally, for GJ 585.1, the only K dwarf in our sample, our $11.7\mu\text{m}$ measurement is above the predicted model photosphere at the 1.5σ level, and may warrant further observations at longer wavelengths. However, given that this is only a 1.5σ excess, we do not believe it is likely to be real.

5. MODELING OF CIRCUMSTELLAR PROCESSES

In section 5.1, we review the current observational knowledge of M dwarf circumstellar environments. In section 5.2, we contrast observations with a steady-state application of P-R grain removal for M Dwarfs. In section 5.3 we present a model for stellar wind drag grain removal for M dwarfs. In section 5.4, we discuss the current knowledge of M dwarf stellar winds. In section 5.5, we then evaluate the relevance of stellar wind drag in M dwarf debris disks and we present a model for their evolution. In section 5.6, we discuss other dust removal mechanisms.

5.1. The Observational Dearth of M Dwarf Debris Disks

Circumstellar disks are common around M Dwarfs younger than ~ 5 Myr; the inner parts of these disks appear to dissipate within 5-10 Myr, and any remaining disks are relatively rare in systems older than 10 Myr. AU Mic (GJ 803) and GJ 182 are the only two M-type dwarfs older than 10 Myrs with an infrared or sub-mm excess, confirmed with ground-based observations, that is indicative of a debris disk (Song et al. 2002; Liu et al. 2004; Zuckerman 2001; Fajardo-Acosta et al. 2000). This lack of late-type dwarfs older than 10 Myrs with an infrared excess does not appear to be a selection effect due to IRAS detection limits but rather an age dependent phenomenon (Song et al. 2002; Song 2003, private comm.).

Weinberger et al. (2004) propose that the lack of warm infrared excesses associated with the inner disks of K and M Dwarfs in the TW Hya association implies rapid planet formation within 5-10 Myrs, which in turn depletes available parent bodies for dust replenishment. For AU Mic, Liu et al. (2004) argue that the lack of warm ($T \sim 200\text{K}$) dust in the inner region of the circumstellar disk suggests the presence of an unseen planetary companion, also indicative of rapid planet formation within ~ 10 Myr.

In support of this rapid planet formation theory, it is known that primordial material to potentially form planets is common around low-mass stars and brown dwarfs with ages less than a few million years (Liu et al. 2003; Klein et al. 2003; Pascucci et al. 2003; Lada et al. 2000; Beckwith et al. 1990; Osterloh & Beckwith 1995). Hen 3-600 (TWA 3, a multiple star system) and TWA 7 are M-type pre-main sequence members of the $\sim 5\text{-}10$ Myr old TW Hydrae Association (Zuckerman 2001). Coku Tau 4, AA Tau and CD $-40^\circ 8434$ are further examples of T Tauri type pre-main sequence M Dwarfs with observed infrared excesses (Metchev et al. 2004; Quillen et al. 2004; Kenyon & Hartmann 1995). However, recent simulations of terrestrial planet formation around solar type stars take on average 10-50 Myrs to accrete into the analogs of our solar system terrestrial planets. This process includes large-scale impacts – like the one that is theorized to have formed Earth’s moon – lasting on the time-scale of ~ 100 Myrs (Agnor et al. 1999) and thus providing parent bodies to generate extrasolar zodiacal clouds on these timescales. The arguments of Weinberger et al. (2004); Song et al. (2002); Liu et al. (2004) lead us to conclude that there potentially exists a different debris disk evolution timescale for K and M Dwarfs, and herein we propose such a mechanism.

5.2. Grain Removal from Poynting-Robertson Drag

The dust we observe in a debris disk is replenished by the grinding (destruction) of parent bodies (Zuckerman 2001), and removed under the action of Poynting-Robertson and other forces. Thus, the infrared excess can be related to the destruction rate of the parent bodies. In a simple model, we derive from Chen & Jura (2001) and Jura (2004) a relation between L_{IR} and the rate at which mass is being removed from parent bodies and converted into dust, \dot{M}_d :

$$\dot{M}_d c^2 = C_0 L_{IR} \quad (1)$$

where C_0 is a numerical constant of order unity, $L_{IR} \approx (\nu L_\nu)_{IR}$ is the luminosity of the dust infrared excess and c is the speed of light. Chen & Jura (2001) used $C_0 = 4$, where C_0 depends upon the assumed initial dust distribution relative to the inner radius at which the

dust sublimates.

We have used the steady-state assumption that $\dot{M}_d = M_{dust}/t_{removal}$ and Equations (4) and (5) in Chen & Jura (2001) to arrive at Equation (1) above. Note that in the derivation of Chen & Jura (2001), the dominant grain removal process is assumed to be Poynting-Robertson (P-R) drag ($t_{removal} = t_{PR}$).

For M-type dwarfs, the characteristic grain removal time-scales from Poynting-Robertson drag are significantly longer than for earlier type dwarfs due to the relatively lower luminosities in late-type dwarfs. Thus, contrary to the observational dearth of M-type debris disks, we might expect a large abundance of dust around these stars.

5.3. Grain Removal from Corpuscular Stellar Wind Drag

We propose that the corpuscular (proton) stellar wind drag, hereafter stellar wind drag, in late-type dwarfs serves as the dominant mechanism for grain removal in these stars, in contrast to the P-R drag cited for earlier-type debris disk evolution. An analogous and more detailed derivation applied to red giants can be found in Jura (2004).

The stellar wind drag force is caused primarily by the proton flux from the solar wind impacting dust grains and the resulting anisotropic recoil; the effect is analogous to the Poynting-Robertson drag (Burns et al. 1979; Gustafson 1994; Holmes et al. 2003). In our own solar system, the solar wind drag has been measured to be on the order of 30% of the Poynting-Robertson drag force, varying in strength between 20% and 43% (Gustafson 1994). Holmes et al. (2003) approximates a value of 1/3.

To first order in v_{orb}/c and v_{orb}/v_{sw} – assuming each of these quantities is $\ll 1$ as in Gustafson (1994), where v_{orb} is the grain orbital velocity of a grain assumed to be in a circular orbit, and where v_{sw} is the proton stellar wind velocity assumed to be entirely radial – we can write the ratio of drag times t_{pr}/t_{sw} in terms of the magnitude of force ratios:

$$\frac{t_{pr}}{t_{sw}} = \left| \frac{\vec{F}_{sw} \cdot \hat{\theta}}{\vec{F}_{PR} \cdot \hat{\theta}} \right| = \frac{c}{v_{sw}} \times \left| \frac{\vec{F}_{sw} \cdot \hat{r}}{\vec{F}_{rad} \cdot \hat{r}} \right| \quad (2)$$

where F_{sw} , F_{rad} , and F_{PR} correspond to the solar wind pressure, radiation pressure and Poynting-Robertson drag forces respectively, and $\hat{\theta}$ and \hat{r} correspond to the azimuthal and radial unit vectors in spherical coordinates. We note that while the radiative stellar wind pressure can be dominated by the radiation pressure, the drag force ratio is enhanced by a factor of c/v_{sw} in favor of the corpuscular drag force. We then write:

$$\frac{t_{pr}}{t_{sw}} = \frac{c}{v_{sw}} \times \frac{Q_{sw}}{Q_{pr}} \left(\frac{\dot{M}_{sw} v_{sw}}{L_*/c} \right) = \frac{Q_{sw}}{Q_{pr}} \frac{\dot{M}_{sw} c^2}{L_*} \quad (3)$$

where properties such as grain size, density and distance from the star drop out from the above expression, and where Q_{sw}/Q_{pr} is the ratio of coupling coefficients. For our own Solar System, taking $\dot{M}_{sw} \sim 2 \times 10^{-14} M_\odot \text{ yr}^{-1}$ and assuming $Q_{sw}/Q_{pr} = 1$, Equation (3) evaluates to 37%.

Equation (3) presents a first-order expression to evaluate the relative importance of the P-R and stellar wind drags; more detailed expressions for the drag forces can be found in (Gustafson 1994). We deduce from Equation (3) that stellar wind drag can dominate P-R drag due to the lower M-dwarf luminosities relative to the Sun. We write a more general expression for the inferred parent body destruction rate in cgs units, \dot{M}_d , by combining Equation (1) and Equation (3):

$$\dot{M}_d = \left(\frac{C_0 L_{IR}}{c^2} \right) \times \left(1 + \frac{\dot{M}_{sw} c^2}{L_*} \right) \quad (4)$$

where we have assumed for simplification and clarity above that $Q_{sw}/Q_{pr} = 1$ and we note again that L_{IR} represents the luminosity of the infrared excess due to dust. We can write the above equation in terms of the observed fractional infrared excess as:

$$\frac{L_{IR}}{L_*} = \frac{\dot{M}_d c^2}{C_0 (L_* + \dot{M}_{sw} c^2)} \quad (5)$$

Equations (4) and (5) limit to the following expressions when stellar wind drag is the dominant grain removal mechanism:

$$\dot{M}_d = \frac{C_0 \dot{M}_{sw} L_{IR}}{L_*} \quad (6)$$

$$\frac{L_{IR}}{L_*} = \frac{\dot{M}_d}{C_0 \dot{M}_{sw}} \quad (7)$$

Scaling the P-R drag timescale (see Equation (5) in Chen & Jura (2001)) by t_{sw}/t_{pr} from the right hand side of Equation (3), we derive the grain removal time-scale for stellar-wind drag:

$$t_{sw} = \frac{4\pi a \rho_{dust} D^2}{3Q_{sw} \dot{M}_{sw}} \quad (8)$$

where D is the distance of the grain from the star.

5.4. Late-Type Dwarf Stellar Winds

Empirical and semi-empirical arguments have shown that late-type dwarf wind mass loss rates can exceed the solar wind mass loss rate of $\sim 2 \times 10^{-14} M_{\odot} \text{ yr}^{-1}$ by factors ranging from ~ 10 (Mullan et al. 1992; Fleming et al. 1995; Wargelin & Drake 2001, 2002; Wood et al. 2001, 2002) to a proposed $\sim 10^4$ in the case of the M dwarf flare-star YZ Cmi (Mullan et al. 1992). This enhanced stellar wind mass-loss is expected due to the hotter coronae and increased magnetic activity in active late-type dwarfs. Recent models suggest that the mass-loss rates from late-type dwarfs are a few times $10^{-12} M_{\odot} \text{ yr}^{-1}$ (Wargelin & Drake 2001; Lim & White 1996; van den Oord & Doyle 1997); this predicted mass loss rate is still a factor of ~ 100 times the solar value.

The task of remotely observing such winds (directly or indirectly) around other solar-type dwarfs has been a substantial challenge. The measurements of wind rates were made indirectly from “astrospheric” absorption high-resolution Hubble Space Telescope spectra of Ly α absorption lines – neutral interstellar hydrogen heated by the presence of a wind and the resulting interaction with the local interstellar medium. From observations of G and K dwarfs, Wood et al. (2002) derived the relationship that $\dot{m}_{sw} \propto F_X^{1.15 \pm 0.20}$ from correlating observed stellar wind mass-loss rates with X-ray activity, where F_X is the X-ray flux at the surface of the star and \dot{m}_{sw} is the mass-loss rate per unit surface area. This relation implies a mass loss rate, \dot{M}_{sw} , ~ 1000 times that of the solar wind for the particular case of AU Mic (Wood et al. 2002; Huensch et al. 1999).

With substantial uncertainty, Wood et al. (2002) derive $\dot{M}_{sw} \approx \dot{M}_{\odot} (t/t_{\odot})^{-2.00 \pm 0.52}$ from stellar rotational velocity evolution and correlation with F_X . Wood et al. (2002) caution that this relation may not accurately extrapolate for stars younger than ~ 300 Myr, but the mass-loss will generally decrease with time from some maximum value. Solar wind mass-loss rates as high as 10^3 times its present value have been hypothesized to account for the required luminosity and corresponding initial solar mass (Sackmann & Boothroyd 2003; Wood et al. 2002), but such a large enhancement in the mass-loss rate may not extend to young M-type dwarfs (Lim & White 1996; van den Oord & Doyle 1997).

5.4.1. Proxima Cen

No one has detected a wind from the nearest M Dwarf, Proxima Cen, but ascribing an appropriate upper-limit is a matter of debate. Wood et al. (2001) placed an upper limit on \dot{M}_{sw} of 0.2 times the solar wind mass-loss rate, contrary to the arguments of Wargelin & Drake (2001); Lim & White (1996); van den Oord & Doyle (1997). However, the assumptions of Wood et al. (2001) about the intrinsic stellar $L\alpha$ line profile are cited as controversial in Wargelin & Drake (2002). From X-ray observations of charge exchange between the wind of Proxima Cen and neutral ISM gas, Wargelin & Drake (2002) instead place a $3\text{-}\sigma$ upper-limit constraint of 14 times the solar wind mass-loss rate, \dot{M}_{sw} . More accurate estimates and measurements of M dwarf wind mass-loss rates will resolve these differences and uncertainties.

5.5. The Relevance of Stellar Wind Drag for M Dwarf Debris Disk Evolution

It seems plausible that M Dwarf wind mass-loss rates can exceed the solar value by at least a factor of 10. Consequently, scaling from Equation (3), we find that stellar wind drag dominates P-R drag in M dwarfs. We can now estimate L_{IR}/L_* when stellar wind drag is the dominant grain removal mechanism. From Equation (7), using $\dot{M}_{sw} = \dot{M}_\odot (t/t_\odot)^{-2.00 \pm 0.52}$ from Wood et al. (2002), estimating $\dot{M}_d = 4 \times 10^6 (t_*/t_\odot)^{-1.76 \pm 0.2}$ g/s, and setting $C_0 = 4$, we calculate:

$$\frac{L_{IR}}{L_*} \sim 9 \times 10^{-7} \left(\frac{t_*}{t_\odot} \right)^{0.24 \pm 0.6} \quad (9)$$

Equation (9) predicts that the frequency of M dwarf debris disks older than ~ 10 Myr is roughly independent of age. Furthermore, the predicted infrared excess ratio is below typical observational limits (Metchev et al. 2004; Spangler et al. 2001; Liu et al. 2004). For our estimate of \dot{M}_d used above, we inferred the time-dependence from Spangler et al. (2001); Liu et al. (2004), and we adopted a proportionality constant of $C_0 L_{IR}/c^2 = C_0 L_* f_d/c^2 = 4 \times 10^6$ g/s from Equation (1). For this proportionality constant for \dot{M}_d , we again set $C_0 = 4$, $L_* = L_\odot$ and we inferred $f_d = 2.5 \times 10^{-7}$ at $t = t_\odot$ from Figure 2 in Spangler et al. (2001). This estimate for \dot{M}_d is consistent with the dust replenishment rate for the zodiacal cloud, $\dot{M}_d \sim 3 \times 10^6$ g/s (Fixsen & Dwek 2002).

5.6. Other Dust Removal Mechanisms

Stellar wind drag can dominate P-R drag in the evolution of M dwarf debris disks when $t_{pr}/t_{sw} > 1$, which occurs when $\dot{M}_{sw}/\dot{M}_{\odot} \gtrsim 3 \times L_*/L_{\odot}$. We can now put this result in context with the role of collisions and the role of grain blowout, both through radiation pressure and stellar wind pressure.

Dust grain blowout due to radiation pressure is irrelevant for M dwarfs, due to the lower luminosity and longer peak wavelength of radiation ($L_* \sim 10^{-1} \dots^{-3} L_{\odot}$, $\lambda_{peak} > 1\mu m$). We present a simplistic spherical grain model to explain this result. Assuming the absorption coupling coefficient $Q_a = 1$ and the average grain density $\rho_{dust} = 2.5 \text{ g cm}^{-3}$, we calculate from Equation (2) in Chen & Jura (2001) a radiative blowout grain size radius, $a_{blowout} \sim 0.1\mu m$ for a M0 dwarf, with $L_* = 0.1L_{\odot}$, $M_* = 0.5M_{\odot}$. Because $2\pi a_{blowout}/\lambda_{peak} < 1$ for all M Dwarfs, our assumption that $Q_a = 1$ is invalid and Equation (2) in Chen & Jura (2001) is not applicable.

When $2\pi a/\lambda < 1$, we write from Equation 7.7 in Spitzer (1998):

$$Q_a(a, \lambda) = -8\pi \text{Im} \left(\frac{n^2 - 1}{n^2 + 2} \right) \frac{a}{\lambda} \quad (10)$$

where n is the complex index of refraction that is material-dependent. Equation (10) evaluates to $Q_a(a, \lambda) \sim a/\lambda$ for various silicates at wavelengths of $\sim 1\mu m$ (Dorschner et al. 1995; Ossenkopf et al. 1992). We integrate $Q_a(a, c/\nu)L_{\nu}$ over ν for a stellar blackbody spectrum and derive $Q_a L_* \sim L_* a/\lambda_{peak}$. The ratio of the radiation pressure to the gravitational attraction is then independent of grain size:

$$\beta \equiv \frac{F_{rad}}{F_{grav}} \approx \frac{3L_*}{16\pi cGM_*\rho_{dust}\lambda_{peak}} \quad (11)$$

where G is Newton's gravitational constant, and c is the speed of light. Taking $\rho_{dust} = 2.5 \text{ g cm}^{-3}$, $L_* = 0.1L_{\odot}$, $M_* = 0.5M_{\odot}$, and $\lambda_{peak} = 1\mu m$, we calculate $\beta \sim 0.05$. We conclude that $\beta \ll 1$ for all M dwarfs – radiation pressure is insufficient to overcome gravitational attraction in expelling orbiting grains of any size. The grain morphology for these small grains can be important relative to the blackbody approximation, and a more detailed calculation of the effective cross section to evaluate the relevance of radiative blowout has been done by Saija et al. (2003). The authors similarly conclude that the radiative pressure for small amorphous grains orbiting a 2700K M dwarf is negligible.

Krist et al. (2005) suggest that stellar wind pressure may play a role in the dissipation of dust around AU Mic. We compute the stellar wind blowout radius to be:

$$a_{blowout} = \frac{3Q_{sw}\dot{M}_{sw}v_{sw}}{16\pi GM_*\rho_{dust}} \quad (12)$$

where v_{sw} is the stellar wind velocity, and any grains smaller than $a_{blowout}$ will be expelled under the action of stellar wind pressure. This can be derived directly by taking the ratio of the stellar wind and gravitational forces and setting them equal to 1, or by multiplying Equation (2) in Chen & Jura (2001) by $|F_{sw}^{\vec{r}} \cdot \hat{r}/F_{rad}^{\vec{r}} \cdot \hat{r}|$ (see Equations (2) and (3)).

For a $0.5M_{\odot}$ M0 dwarf with a solar mass-loss rate and solar wind velocity of ~ 400 km/s (Feldman et al. 1977), assuming $Q_{sw} = 1$ and $\rho_{dust} = 2.5$ g cm $^{-3}$, the corresponding blowout radius is insignificant at $2 \times 10^{-4} \mu m$. However, for a $0.5M_{\odot}$ M0 dwarf with a mass-loss rate of $\sim 10^3 \dot{M}_{\odot}$, the corresponding blowout radius would be $0.2 \mu m$, increasing to $0.9 \mu m$ for a $0.1M_{\odot}$ late-M dwarf with a mass-loss rate of $\sim 10^3 \dot{M}_{\odot}$. Thus, the relevance of stellar wind blowout increases for later spectral types, but is only relevant for extremely young or active M Dwarfs with potentially unrealistic mass-loss rates. The validity of our assumption that $Q_{sw} = 1$ for these grain sizes is also uncertain.

Dominik & Decin (2003) suggest that all the known debris disk systems are collision-dominated and not P-R drag dominated. This relies on the assumption that dust grains can be ground down by collisions until they are blown out by radiation pressure on a time-scale short compared to a drag time-scale. This assumption does not hold for M Dwarf debris disks, since dust grains are not blown out by radiation pressure. While M dwarf debris disks will be collisionally processed on short time-scales, stellar wind drag or grain growth is likely to still be the dominant grain removal process. This modification predicts an excess of small grains for M dwarf debris disks relative to those around earlier-type stars and hence a relatively blue disk color.

6. DISCUSSION

6.1. Some Implications of Stellar Wind Drag for M Dwarfs

The time-dependence and steady-state assumptions of Equation (9) may be oversimplified, and the normalization is similarly uncertain by at least a factor of two. Nonetheless, stellar wind drag offers an explanation for the lack of M-type debris disks older than 10 Myrs identified in Song et al. (2002); Fajardo-Acosta et al. (1999); Mamajek et al. (2004). For the late-type dwarfs with confirmed infrared excesses in Metchev et. al. (2004), the estimated disk masses derived from the Chen & Jura (2001) model should be adjusted higher by the ratio of t_{pr}/t_{sw} . For the late-type dwarfs in the TW Hydrae association, the removal of

grains by the stellar wind drag offers an alternative explanation to rapid planet formation put forth by Weinberger et al. (2004). The circumstellar disks and forming planetesimals may still exist, but the infrared excess emission can be effectively “surpressed” by the stellar wind drag relative to the effects of the Poynting-Robertson drag. When gas is still present in the disk, the dynamics are more complicated and our model does not apply.

6.2. AU Mic: An Application of the Model

AU Mic is the only M-dwarf with an imaged circumstellar disk and infrared excess older than 10 Myr. We propose that stellar wind drag offers an alternative explanation for the lack of warm dust grains observed near AU Mic. The observed substructure and turnover in the slope of the radial surface brightness profile are naturally explained by the presence of a planetesimal disk in the inner ~ 35 AU Metchev et al. (2005); Krist et al. (2005); Liu (2004). This inner disk could be produced by the stochastic destruction of parent-bodies, the subsequent generation of dust, and the removal of the dust by stellar wind drag within a time short compared to the ~ 12 Myr age of AU Mic. If circumstellar gas is present in the AU Mic disk, the physical interpretation becomes more complicated and our model does not apply.

We can estimate grain removal time-scales from Equation (8). We assume a grain size of $a = 0.5\mu\text{m}$ (Metchev et al. 2005), a grain density of $\rho_s = 2.5 \text{ g cm}^{-3}$, and $Q_{sw} = Q_{pr} \sim 1$. Since these assumptions dictate the grain opacity, which is unknown to within an order of magnitude, our estimates are similarly uncertain. For AU Mic, we could take $\dot{M}_{sw} \sim 10^3 \dot{M}_\odot$ from the X-ray luminosity (Wood et al. 2002; Huensch et al. 1999). However, this is a factor of 5-10 higher than the maximum \dot{M}_{sw} inferred from modeling M dwarf winds (Wargelin & Drake 2001; Lim & White 1996; van den Oord & Doyle 1997). Thus, our estimate for \dot{M}_{sw} is also uncertain by an order of magnitude, and we instead adopt $\dot{M}_{sw} = 10^2 \dot{M}_\odot$ for this calculation. If $\dot{M}_{sw} = 10^2 \dot{M}_\odot$, then stellar wind drag removes grains smaller than $0.5\mu\text{m}$ in the inner 35AU of the AU Mic disk within $\sim 4 \times 10^4 \text{ yr}$. Similarly, grains smaller than $0.5\mu\text{m}$ will be removed out to 250AU in $\sim 2 \text{ Myr}$. We deduce that at least the inner portion of the AU Mic debris disk must have been replenished by collisions of parent bodies. Neglecting stellar wind drag for comparison and assuming $L_* = 0.13L_\odot$ (Metchev et al. 2005), P-R drag would remove grains smaller than $0.5\mu\text{m}$ out to ~ 35 AU in ~ 8 Myr.

If $\dot{M}_{sw} = 10^3 \dot{M}_\odot$, we calculate a corresponding stellar wind blowout radius of $0.2\mu\text{m}$ from Equation (12), where we assume $Q_{sw} = 1$, $\rho_{dust} = 2.5 \text{ g cm}^{-3}$, $M_* = 0.5M_\odot$, and $v_{sw} = v_{sw,\odot} = 400 \text{ km/s}$. This is consistent with the minimum grain radius of $0.3\mu\text{m}$ derived observationally by Metchev et al. (2005) at a distance of 50-60AU. This implies there will be

a relatively large number of grains less than $1\mu\text{m}$ in size in the AU Mic disk, since such grains are too large to be blown out by stellar wind pressure and radiation pressure is negligible. This is consistent with the observed overall blue color of the AU Mic disk relative to the colors of disks around earlier-type stars (Metchev et al. 2005; Krist et al. 2005).

Equation (9) predicts that $L_{IR}/L_* \sim 2 \times 10^{-7}$ for AU Mic, although we caution against applying Equation (9) to stars as young as AU Mic. Liu et al. (2004) measure $L_{IR}/L_* \sim 6 \times 10^{-4}$, a factor of 3×10^3 higher, from infrared and sub-mm observations. This implies that the AU Mic disk is not in a steady-state; leftover primordial material or a recent major planetesimal collision contributing to the observed dust excess could be considered “transient” effects.

7. CONCLUSIONS

We do not observe any excess $11.7\mu\text{m}$ emission for nine late-type dwarfs, selected for their youth or apparent IRAS $12\mu\text{m}$ excess. We find that stellar wind drag can dominate the Poynting-Robertson effect in grain removal from late-type dwarf debris disks, and this offers an explanation for the dearth of known M Dwarf systems older than 10 Myrs with infrared excesses. We predict that M Dwarf debris disks older than 10 Myr will have a roughly equal age distribution, with $L_{IR}/L_* \sim 10^{-6}$. Future efforts, such as the Spitzer Space Telescope, may be successful in detecting these systems.

7.1. Acknowledgements

The authors wish to recognize and acknowledge the very significant cultural role and reverence that the summit of Mauna Kea has always had within the indigenous Hawaiian community. We are most fortunate to have the opportunity to conduct observations from this mountain.

This publication makes use of data products from the Two Micron All Sky Survey, which is a joint project of the University of Massachusetts and the Infrared Processing and Analysis Center/California Institute of Technology, funded by the National Aeronautics and Space Administration and the National Science Foundation.

This research has made use of the SIMBAD database, operated at CDS, Strasbourg, France. This research has made use of the VizieR catalogue access tool, CDS, Strasbourg, France.

Thanks to Michael Liu, Ben Zuckerman, Inseok Song, Paul Kalas, Alycia Weinberger, Christine Chen, Stanimir Metchev and Thayne Currie for their insightful conversations and comments. This work is supported by NASA.

REFERENCES

- Agnor, C., Canup, R., & Levison, H., 1999, *Icarus*, 142, 219
- Amado, P. & Byrne, P., 1997, *A&A*, 319, 967
- Aumann, H. & Probst, R., 1991, *ApJ*, 368, 264
- Backman, D., & Paresce, F., in *Protostars and Protoplanets III*, Levy, E. & Lunine, J., Eds., 1993, 1253
- Beckwith, S. et al., 1990, *AJ*, 99, 924
- Beichman, C. et al., 1988, *IRAS Explanatory Supplement*
- Bond, I. et al., 2004, *ApJ*, 606, L155
- Burns, J., Lamy, P., & Soter, S., 1979, *Icarus*, 40,1
- Butler P. et al., 2004, *ApJ*, 617, 580
- Chen, C. & Jura, M. 2001, *ApJ*, 560, L171
- Chyba, C., 1991, *Icarus*, 92, 217
- Cohen, M., Wheaton, W., & Megeath, S., 2003, *AJ*, 126, 1090
- Cutri, R. et al., 2003, *Explanatory Supplement to the 2MASS All Sky Data Release*
- D'Antona, F. & Mazitelli, I., 1997, *Mem. S.A.It.*, 68,4, 807
- Decin, G. & Dominik, C., 2003, *ApJ*, 598, 636
- Dominik, C. & Decin, G., 2003, *ApJ*, 598, 626
- Dorschner, J. et al., 1995, *A&A*, 300, 503
- Drilling, J. & Landolt, A., 2000, in *Allens Astrophysical Quantities*, ed. A. N. Cox (New York: Springer), 389
- Fajardo-Acosta, S., Beichman, C., & Cutri R., 2000, *ApJ*, 538, L155
- Fajardo-Acosta, S., Beichman, C., & Cutri, R., 1999, *ApJ*, 520, 215
- Feldman, W. et al., 1977, in *The Solar Output and its Variation*, ed. O. White (Boulder: Colorado Associated Univ. Press), 351

- Fixsen, D. & Dwek, E., 2002, ApJ, 578, 1009
- Fleming, T., Schmitt, J., & Giampapa, M., 1995, ApJ, 450, 401
- Gaidos, E. & Koresko, C., New Astronomy, 2004, Vol. 9, Issue 1, 33-42.
- Gizis, J., Reid, I.N., & Hawley, S., 2002, AJ, 123, 3356
- Gliese, W. & Jahreiss, H., 1979, A&AS, 38, 423
- Gliese, W. & Jahreiss, H., 1991, *Preliminary Version of the Third Catalogue of Nearby Stars*
- Gorjian, V., 2003, private comm.
- Gustafson, B., 1994, Annu. Rev. Earth Planet. Sci., 22, 553
- Habing, H. et al., 2001, A&A, 365, 545
- Hauschildt, P. et al., 1999, ApJ, 512, 377
- Holmes, E. et al., 2003, ApJ, 597, 1211
- Houdebine, E., et al., 1996, A&A, 305,209
- Huensch, M. et al., 1999, A&AS, 135, 319
- Jones, B. & Puetter, R., 1993, Proc. SPIE, 1946, 610
- Jura, M., 2004, ApJ, 603, 729
- Kalas P., Liu, M., & Matthews, B., 2004, Science, 303, 1990.
- Kastner, J. et al, 2003,ApJ, 585, 878
- Kenyon, S., & Hartmann, L.,1995,ApJS, 101, 117
- Klein, R. et al., 2003, ApJ, 593, L57
- Krist, J. et al., 2005, AJ, 129, 1008
- Lada, C. et al., 2000, AJ, 120, 3162
- Laughlin, G., Bodenheimer, P., & Adams, F.,2004,ApJ, 612, L73
- Lim, J. & White, S., 1996, ApJ, 462, L91
- Liu, M., 2004, Science, 305, 1442

- Liu, M. et al., 2004, *ApJ*, 608, 526.
- Liu, M., Najita, J., & Tokunaga, A., 2003, *ApJ*, 585, 372
- Mamajek, E. et al., W., 2004, *ApJ*, 612, 496
- Marcy, G. et al., 2001, *ApJ*, 556, 296
- Marcy, G. et al., 1998, *ApJ*, 505, L147
- Mathioudakis, M. & Doyle, J., 1993, *A&A*, 280, 181
- Matthews, K. & Soifer, T., 1994, in *Infrared Astronomy with Arrays: the Next Generation*, ed. I. McLean (Dordrecht: Kluwer), 239
- Mayor, M. & Queloz, D., 1995, *Nature*, 378, 355
- Metchev, S. et al., 2005, *ApJ*, 622, 451
- Metchev, S., Hillenbrand, L., & Meyer, M., 2004, *ApJ*, 600, 435
- Monet, D. et al., 1998, *USNO-A V2.0, A Catalog of Astrometric Standards*
- Mullan, D. et al., 1992, *ApJ*, 397, 225
- Mullan, D. et al., 1989, *ApJ*, 343, 400
- Ney, E., 1982, in *Comets*, ed. L. Wilkening, University of Arizona, Tucson, 323
- Noci, G., 1988, in *Mass Outflows from Stars and Galactic Nuclei*, ed.s L. Branichi & R. Gilmozzi (Dordrecht: Kluwer), 11
- Ochsenbein F., Bauer P., & Marcout J., 2000, *A&AS*, 143, 221
- Ossenkopf, V. et al., 1992, *A&A*, 261, 567
- Osterloh, M. & Beckwith, S., 1995, *ApJ*, 439, 288
- Pascucci, I. et al., 2003, *ApJ*, 590, 111
- Pizzolato, N. et al., 2003, *A&A*, 397, 147
- Quillen, A. et al., 2004, *ApJ*, 612, 137
- Sackmann, I-J. & Boothroyd, A., 2003, *ApJ*, 583, 1024
- Saija, R. et al., 2003, *MNRAS*, 341, 1239

- Song, I. et al., 2002, *AJ*, 124, 514
- Song, i., 2003, private comm.
- Spangler, C. et al., *ApJ*, 555, 932
- Spitzer, L., in *Physical Processes in the Interstellar Medium*, 1998, 151
- Stelzer, B., & Neuhauser, R., 2001, *A&A*, 377, 538
- Stern, R. et al., 1995, *ApJ*, 448, 683
- Terndrup, D. et al., 2000, *AJ*, 119, 1303
- van den Oord, G. H. J. & Doyle, J., 1997, *A&A*, 319, 578
- Walter, F. & Barry, D., 1991, in *The Sun in Time*, eds. C.P. Sonnet et al., University of Arizona, Tuscon, 633
- Wargelin, B. & Drake, J., 2002, *ApJ*, 578, 503
- Wargelin, B. & Drake, J., 2001, *ApJ*, 546, L57
- Weinberger, A. et al., 2004, *ApJ*, 127, 2246
- Wolszczan, A., & Frail, D., 1992, *Nature*, 355, 145
- Wood, B. et al., J., 2002, *ApJ*, 574, 412
- Wood, B. et al., 2001, *ApJ*, 547, L49
- Wilson, R., 1990, *ApJ*, 356, 613
- Zuckerman, B., 2001, *ARA&A*, 39, 549
- Zuckerman, B. et al., 2001, *ApJ*, 562, L87

TABLES

Table 1. Extrasolar Zodiacal Dust

<i>Name</i>	$T_{eff}^{(1)}$ (K)	$D^{(2)}$ (pc)	$F_{11.7\mu m, obs.}$ (mJy)	$F_{IRAS\ 12\mu m}^{(3)}$ (mJy)	$F_{11.7\mu m, mod.}$ (mJy)	$F_{d,\nu}/F_{*,\nu}^{(4)}$
GJ 3136	3200	14.3 ± 2.9	43 ± 8	–	48 ± 2	< 0.56
GJ 3305	3700	$29.8 \pm 0.3^{(5)}$	106 ± 19	–	103 ± 2	< 0.54
GJ 3304	3100	10.0 ± 1.7	50 ± 9	–	61 ± 2	< 0.54
GJ 507.1	3600	19.8 ± 4.3	98 ± 3	166 ± 23	109 ± 3	< 0.09
GJ 585.1	$4200^{(6)}$	25.6 ± 1.1	62 ± 5	106 ± 18	53 ± 2	< 0.24
G 203-047	3200	7.3 ± 0.5	122 ± 5	135 ± 15	125 ± 4	< 0.12
GJ 729	3100	2.97 ± 0.02	373 ± 8	392 ± 74	382 ± 14	< 0.06
GJ 4068	3100	18.2 ± 4.3	$22 \pm 12^{(7)}$	102 ± 8	30 ± 1	< 1.64
HU Del	3000	8.9 ± 0.2	55 ± 3	89 ± 16	59 ± 3	< 0.16

¹ From reduced χ^2 fit of PHOENIX NextGen model spectra to nearest 100 K.

² Inferred from parallax obtained through SIMBAD and VizieR unless otherwise noted.

³ Color-corrected as described in section 2.3, taken from the IRAS Faint Source Catalogue and Point Source Catalogue where available.

⁴ $3\text{-}\sigma$ upper limits inferred from $11.7\mu m$ observations as a function of frequency, ν .

⁵ Zuckerman et al. (2001); Inferred from SIMBAD parallax for primary companion, 51 Eri.

⁶ Model spectra fitted to $\pm 200K$. The best fit temperature is consistent with this source’s previously identified spectral type, K5.

⁷ The error quoted for this particular flux measurement is dominated by systematic error in our calibration rather than statistical uncertainties in the detection itself. Thus we report a detection rather than an upper-limit.

Table 2. Journal of 11.7 μ m Observations

<i>Name</i>	<i>Date Observed (HST, night of)</i>	<i>Integration Time (sec)</i>
GJ 3136	12/20/2002	120
GJ 3305	12/20/2002	120
GJ 3304	12/20/2002	120
GJ 507.1	4/23/2003	240
GJ 585.1	4/23/2003	300
G 203-047	4/23/2003	300
GJ 729	4/23/2003	144
GJ 4068	4/23/2003	120
HU Del	4/23/2003	120

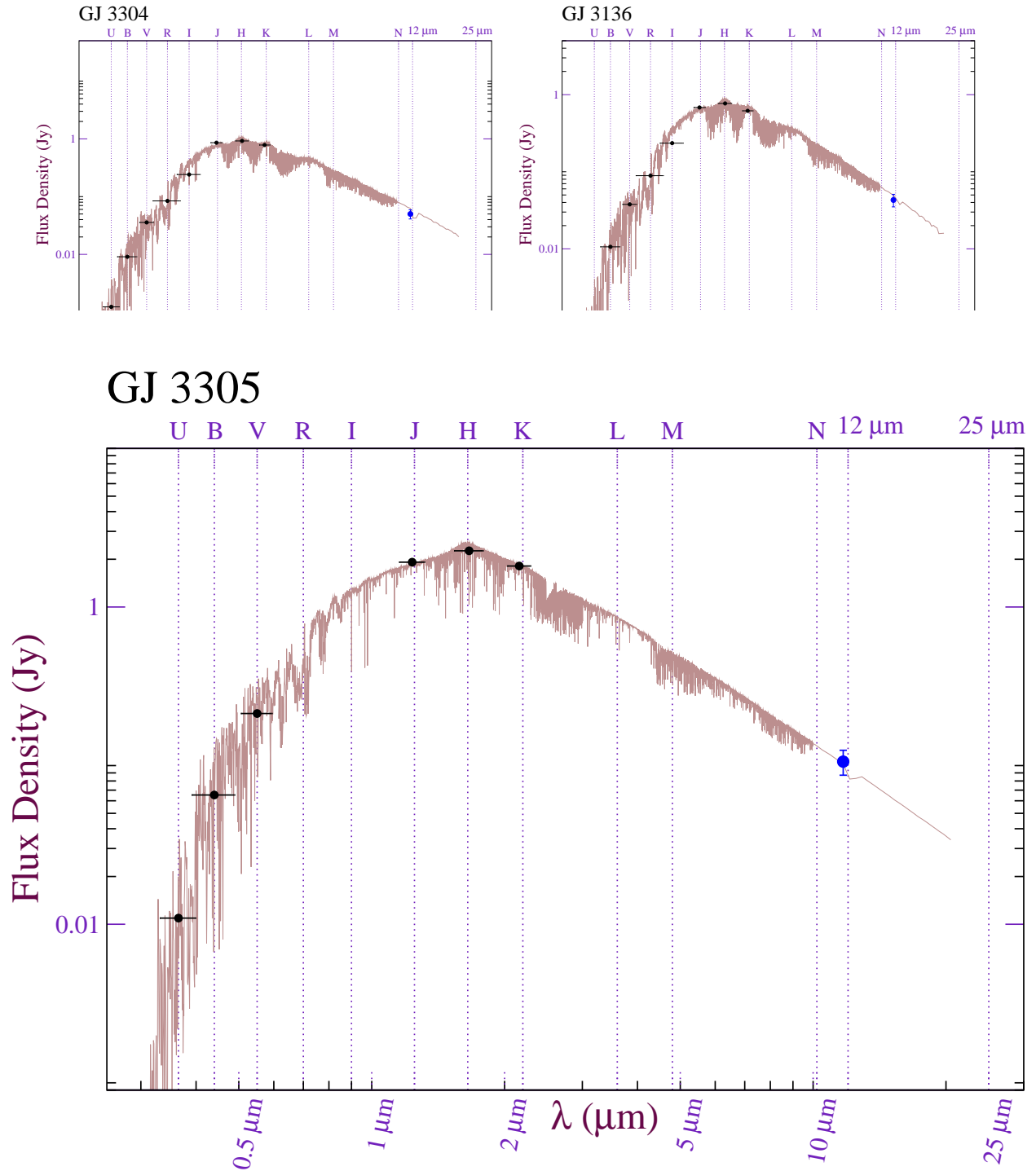


Fig. 1.— Model spectral fits, photometric data and observations, December 2002. Available UBVR_sIJK_s photometry and bandpasses are displayed in black. 11.7 μm observations shown with error bars in blue. Model spectra are displayed in brown.

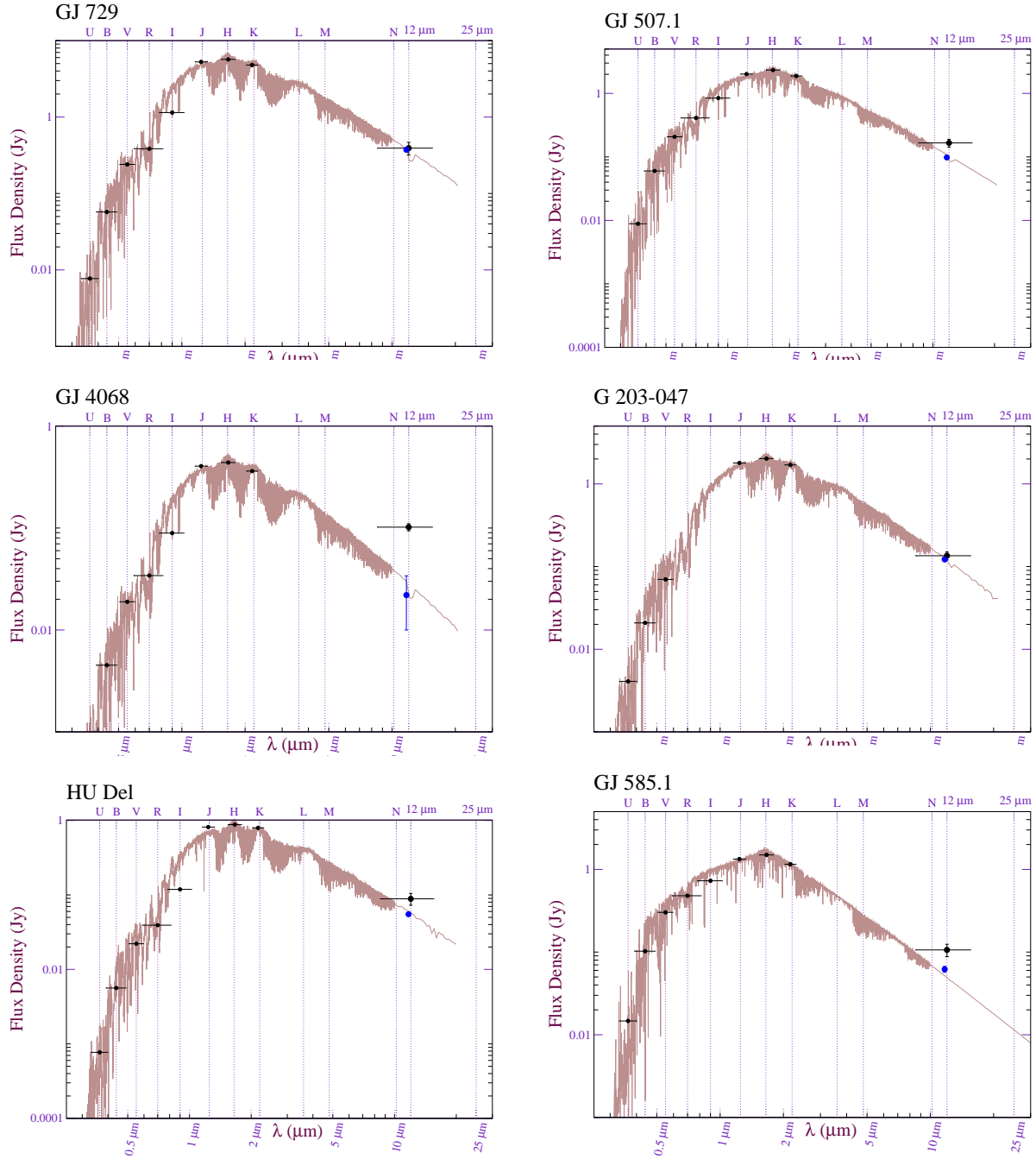


Fig. 2.— Model spectral fits, photometric data and observations, April 2003. Available UBVRIJHK_s photometry and bandpasses are displayed in black. 12 μm IRAS measurements, color-corrected, are also displayed in black with effective bandpass and errors shown. 11.7 μm observations shown with error bars in blue. Model spectra are displayed in brown. See text for discussion.